Journal of Urban and Environmental Engineering
E-ISSN: 1982-3932
celso@ct.ufpb.br
Universidade Federal da Paraíba
Brasil

Chen, Gang; Niu, Yue; Wang, Boya; Tawfiq, Kamal
COLLOID RELEASE FROM DIFFERENT SOIL DEPTH
Journal of Urban and Environmental Engineering, vol. 7, núm. 2, 2013, pp. 223-230
Universidade Federal da Paraíba
Paraíba, Brasil

Journal of Urban and Environmental Engineering, v.7, n.2, p.223-230

ISSN 1982-3932
doi: 10.4090/juee.2013.v7n2.223230

Journal of Urban and Environmental Engineering

www.journal-uee.org

COLLOID RELEASE FROM DIFFERENT SOIL DEPTH

Gang Chen[1*], Yue Niu[2], Boya Wang[1] and Kamal Tawfiq[1]

[1]*Department of Civil Engineering and Environmental Engineering, FAMU-FSU College of Engineering, United States*

[2]*Qingdao Drainage Management Bureau, Qingdao, P.R. China*

Received 04 February 2013; received in revised form 2 September 2013; accepted 6 September 2013

Abstract: Naturally occurring clay colloidal particles are heavily involved in sediment processes in the subsurface soil. Due to the importance of these processes in the subsurface environment, the transport of clay colloidal particles has been studied in several disciplines, including soil sciences, petrology, hydrology, etc. Specifically, in environmental engineering, clay colloid release and transport in the sediments have been extensively investigated, which are motivated by environmental concerns such as colloid-facilitated contaminant transport in groundwater and the subsurface soil. Clay colloid release is resulted from physical alteration of subsurface sediments. Despite the potential importance of clay colloid activities, the detailed mechanisms of release and transport of clay colloidal particles within natural sediments are poorly understood. Pore medium structure, properties and flow dynamics, etc. are factors that affect clay colloid generation, mobilization, and subsequent transport. Possible mechanisms of clay colloid generation in the sediments include precipitation, erosion and mobilization by changes in pore water chemistry and clay colloid release depends on a balance of applied hydrodynamic and resisting adhesive torques and forces. The coupled role of pore water chemistry and fluid hydrodynamics thus play key roles in controlling clay colloid release and transport in the sediments. This paper investigated clay colloidal particle release and transport, especially the colloidal particle release mechanisms as well as the process modeling in the sediments. In this research, colloidal particle release from intact sediment columns with variable length was examined and colloidal particle release curves were simulated using an implicit, finite-difference scheme. Colloidal particle release rate coefficient was found to be an exponential function of the sediment depth. The simulated results demonstrated that transport parameters were not consistent along the depth of the sediment profile.

Keywords: Colloidal particle release; capillary force; water content; air-water interface

[*] Correspondence to: Gang Chen, Tel.: +1 850 410 6303; Fax: +1 850 410 6142.
E-mail: gchen@eng.fsu.edu

INTRODUCTION

Colloidal particles are defined as small discrete solid-like particles indigenously present in natural porous media, which can be mobilized by means of hydrodynamic and other forces (Bergendahl and Grasso, 2000; Shang *et al.*, 2008). These small colloidal-size range particles are mostly composed of clay minerals (McCarthy and Shevenell, 1998). Several potential sources of mobile colloidal particles in the subsurface media have been identified, including in situ mobilization of particles that are naturally present, formation of colloidal particles by precipitation from super-saturated solutions, and direct introduction of colloidal particles into the subsurface (Thomas and Chrysikopoulos, 2010; Thompson and Scharf, 1994). The colloidal particles generally possess electric charge on their surfaces with dimensions of micrometers, which makes the colloidal particles play important roles in many natural and engineered systems. In natural systems, colloidal particles present a potential health risk due to their propensity to associate with contaminants (Molin and Cvetkovic, 2010; Molin *et al.*, 2010; Sen, 2011). If stable in solution, these colloidal particles and any co-adsorbed contaminants can be transported significant distances (Bolshov *et al.*, 2011; Chen *et al.*, 2005). Colloidal particle release and transport are controlled by their interactions with the surrounding environment. Although colloidal particle interactions have been studied for many years and much has been learned about the physical and chemical processes that determine colloidal particle interactions, there still remains significant uncertainty about the processes that govern colloidal particle release and transport in the subsurface environment.

Under steady and uniform flow, colloidal particle release can be linked to hydrodynamic forces and Derjaguin and Landau, Verwey and Overbeek (DLVO) forces. The statics of the release process has been analyzed for fine particles adhering to a pore surface using balanced hydrodynamic forces and DLVO forces to satisfactorily describe the conditions necessary for colloidal particle release (Bin *et al.*, 2011; Roy and Dzombak, 1996). It is believed that the torque due to the physical perturbation causes the colloidal particles attached to the matrix surface to roll along the surface and release (Shang *et al.*, 2008). Subsequently, colloidal particle detachment and release under water unsaturated conditions can be described by the torque balance (Sharma *et al.*, 1992) as shown in **Eq. (1)**:

$$1.399F_s\frac{H}{2} = (F_{cap} - F^{EL})R\sin\phi \qquad (1)$$

where F_s is the shear force (N), H is the water film thickness (m), F_{cap} is the capillary force (N), ϕ is the critical filling angle (degree), and $R\sin\phi$ is the radius of the contact area on which the capillary force acts (m). The shear force, F_s, is calculated using **Eq. (2)** (Sharma *et al.*, 1992):

$$F_s = 1.7(6\pi)\mu\frac{H}{2}v \qquad (2)$$

where μ is water dynamic viscosity (Ns/m^2) and v is the fluid velocity measured at the distance H/2 from the surface of the pore wall. If the colloidal particle is completely covered with water, then H/2=R. It is usually approximated that the fluid velocity v is the same as the pore water velocity.

Colloidal particle release and subsequent transport are usually described by the advection-dispersion equation (ADE) with colloidal particle release formulated as first-order kinetics (Gravelle *et al.*, 2011; Ryan and Gschwend, 1994). Successful applications of these types of models have been observed in laboratory columns (Roy and Dzombak, 1996). Most of these models are based on the ADE under steady-state saturated flow conditions. In above models, colloidal particle release rate is usually considered to be constant along the depth of the sediments, which is true under high water saturation conditions (Roy and Dzombak, 1996; Shen *et al.*, 2007; Vendelboe *et al.*, 2011). Consequently, colloidal particle concentration would display an exponential increase with the travel distance. However, a growing body of laboratory-scale column experiments suggested that the colloidal particle concentration profiles increased non-exponentially under low water saturation conditions (Bradford *et al.*, 2003; Bradford *et al.*, 2002). Reported differences in colloid profile shape under low water saturation conditions indicate uneven water saturation as well as uneven colloidal particle release along the column length (Li *et al.*, 2004; Bradford and Toride, 2007; Sharma *et al.*, 2008; Tufenkji *et al.*, 2003). Therefore, above models should be modified to reflect variations of colloidal particle release with respect to water saturation.

The aim of this study was to investigate the release of in situ colloidal particles from sediments as a function of sediment depth. In this research, colloidal particle release from intact sediment columns with variable length was explored. It was hypothesized that water saturation varied along the length of the column, leading to variable colloidal particle release. Colloidal particle release and transport were simulated using an implicit, finite-difference scheme and the simulated results demonstrated that colloidal particle release was a function of water saturation in the column.

MATERIALS AND METHOD

Colloidal particle release and mobilization were evaluated in intact sediment columns collected from agricultural soils in Gadsden County of Florida. Soil size and size distribution of the sediment samples were quantified by sieve analysis and the soil water retention properties and hydraulic conductivity were measured using a pressure plate. Sediment columns with different lengths (10.0-cm ID × 10.0-cm length, 10.0-cm ID × 20.0-cm length and 10.0-cm ID × 30-cm length) were used in this study. The sediment columns were obtained by gently hammering PVC columns with fitted circular metal cutting edges down into the soil while they were being held vertical by metal-banded hoops. In order to detect compaction, the vertical distance between the top edge of the columns and the inside soil surface was measured and compared to the vertical distance between the top edge of the columns and the outside soil surface prior to the extraction of each sediment column. No compaction was detected. Soil was then gently removed from around the columns for the column extraction. Once intact sediment columns were extracted, metal cutting edges were removed and end fittings were mounted. The column experiments were conducted under water unsaturated conditions with the columns vertically oriented. Along the length of the columns, tensiometers were evenly mounted. Depending on the length of the column, 1, 2 and 3 tensiometers were mounted to the 10, 20 and 30-cm length columns, respectively. For each run of the column experiments, nano-pure de-ionized water was applied using a sprinkler from the top by a peristaltic pump (Masterflex, Cole-Parmer, Vernon Hills, IL) at an irrigation rate of 100 ml/min. The eluate was collected by a hanging water column in a fraction collector. The colloidal particle concentration was measured using a spectrophotometer against a calibration curve generated using the in situ colloidal particle concentration as the reference.

During the experiments, matric potential inside the columns was monitored and recorded using a Campbell Scientific CR-7X datalogger (Campbell Scientific, Inc., Logan, Utah). Water content within the columns was predicted by fitting the van Genuchten equation (Toride *et al.*, 1995) described by **Eq. (3)**:

$$S_e = [1 + (\alpha h)^n]^{(1/n-1)} \quad (3)$$

where S_e is the effective saturation, α is the inverse of the air-entry potential (cm^{-1}), h is the water potential (cm-H_2O), and n is the parameter related to pore size distribution. Using pressure-plate measurements, α and n were determined to be 0.136 cm^{-1} and 4.776. The effective saturation, S_e, is based on the water volumetric content (Toride *et al.*, 1995) and can be calculated using **Eq. (4)**:

$$S_e = \frac{\theta - \theta_r}{\theta_s - \theta_r} \quad (4)$$

where θ is the volumetric water content (cm^3/cm^3), θ_r is the residual water content (cm^3/cm^3), and θ_s is the saturated water content (cm^3/cm^3). Using pressure-plate measurements, θ_s and θ_r were found to be 0.389 and 0.058 respectively.

Colloidal particle release was controlled by kinetic desorption and colloidal particle transport was subject to deposition (Bradford *et al.*, 2003; Bradford *et al.*, 2002; Lenhart and Saiers, 2002). This process can be described by **Eqs (5)** and **(6)**:

$$\frac{\partial}{\partial t}[\theta C] + \frac{\rho_b S}{S_e}\frac{\partial C_s}{\partial t} = \frac{\partial}{\partial z}[D_z \theta \frac{\partial C}{\partial z}] - \frac{\partial}{\partial z}[qC] - k_1 \theta C \quad (5)$$

$$\frac{\partial C_s}{\partial t} = k_1 \frac{\theta S_e}{\rho_b S_0} C - \beta C_s \quad (6)$$

where C is the colloidal particle concentration in the liquid phase (g/m^3), C_s is the colloidal particle concentration on the sediments (g/g), t is time (sec), D_z is the apparent dispersion coefficient (m^2/s), q is the specific flow rate, i.e., Darcian fluid flux (m/sec), ρ_b is the bulk density (g/m^3), z is the coordinate parallel to the flow (m), S_0 is the air-water interfacial area (m^2/m^3), k_1 is the first order colloidal particle deposition rate coefficient (min^{-1}), and β is the first-order colloidal particle release rate coefficient (min^{-1}).

For colloidal particle release, a constant flux was used for the upper boundary, i.e., $J_w C(0,t)=0$, and a zero gradient was assumed for the lower boundary, i.e., $\theta D_z \partial C / \partial z = 0$. The initial conditions for colloidal particle release were $C(x,0)=0$ and $C_s(x,0)=C_{s_0}$. For matric potential, J_w was used for the upper boundary and a constant potential of -10 cm-H_2O was set for all times as the bottom boundary condition. For each series of the column experiments, a fresh column was used. For colloidal particle release simulations, the initial colloid source C_{s_0} for each breakthrough curve was obtained by integrating the experimental breakthrough curves to obtain the total amount of colloidal particles eluted.

RESULTS AND DISCUSSION

The infiltration event was followed by a steady state flow phase, where matric potential remained constant for the sensors along the length of the columns as shown in **Fig. 1**. In **Fig. 1**, the x-axis represents pore volume in units of 330, 660 and 990 cm^3 for the sediment column length of 10, 20, and 30 cm respectively. That is, 1 pore volume in **Fig. 1** (a, b, c) is equal to 330, 660, and 990 cm^3, respectively. In this research, one tensiometer was built in the middle of every 10-cm length of the sediment columns. Based on the steady-state matric potentials readings, the corresponding effective water saturation was calculated according to the van Genuchten equation, which was 0.89 for the 10-cm column, 0.92 and 0.77 for the 20-cm column, and 0.86, 0.70 and 0.54 for the 30-cm column along the length of the columns from the top to the bottom, respectively. These data demonstrated that water content was not uniform in the columns and the columns had greater effective water saturation at the top and less effective water saturation at the bottom (**Fig. 2**).

Corresponding to the infiltration, colloidal particles were observed to be released and mobilized. When water front reached the bottom of the columns, in situ colloidal particles were observed in the effluent (**Fig. 3**). The colloidal particle breakthroughs coincided with the arrival of the infiltration front at the bottom of the columns. The in situ colloidal particle release and mobilization curves were characterized by a self-sharpening front, which became broader and diffuser at the elution limb. The long-lasting tails of the curves indicated kinetically controlled colloidal particle release from the sediments in the columns. By integrating the colloidal particle breakthrough curves, the amount of in situ colloidal particles released for the irrigation period of the experiment was obtained and used as the initial colloidal particle source to estimate the colloidal particle release rate coefficient.

Mathematical models for colloidal particle release and retention are based on the assumption that colloidal particle release undergoes first order release kinetics and colloidal particle deposition in the porous sediments is described by the filtration theory (Lenhart and Saiers, 2002; Lenhart and Saiers, 2003). In these models, colloidal particle release rate coefficient and deposition rate coefficient are usually assumed to be constant along the depth of the sediments, which is true under favorable release and attachment conditions (Lenhart and Saiers, 2002; Lenhart and Saiers, 2003). Consequently, colloidal particle concentration would display an exponential function with the travel distance. Reported differences in colloid profile shape under unfavorable release and attachment conditions indicated variable colloid release and deposition along soil depth (Li *et al.*, 2004; Bradford and Toride, 2007).

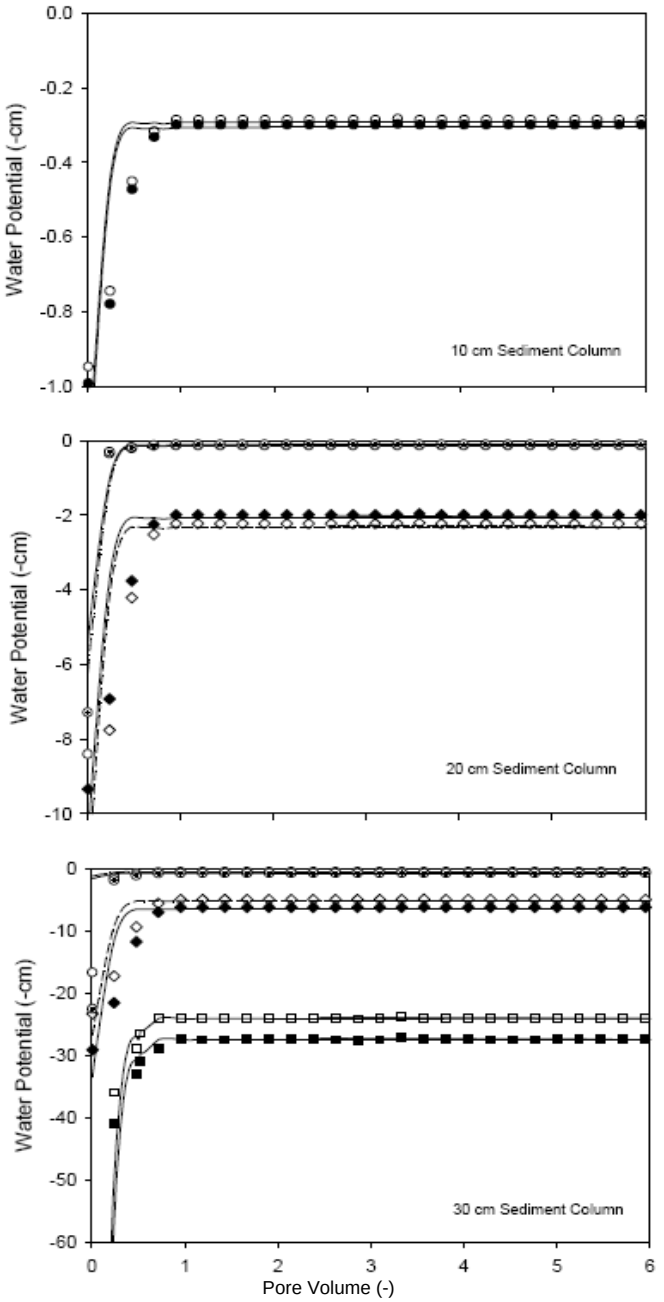

Fig 1. System Matric Potential

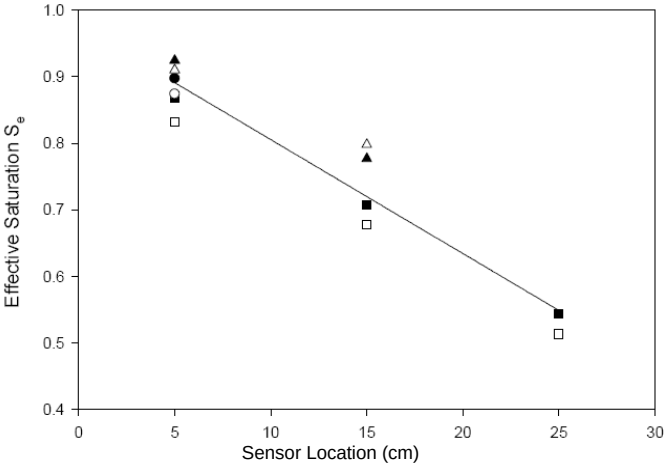

Fig 2. Effective Saturation at Sensor Locations.

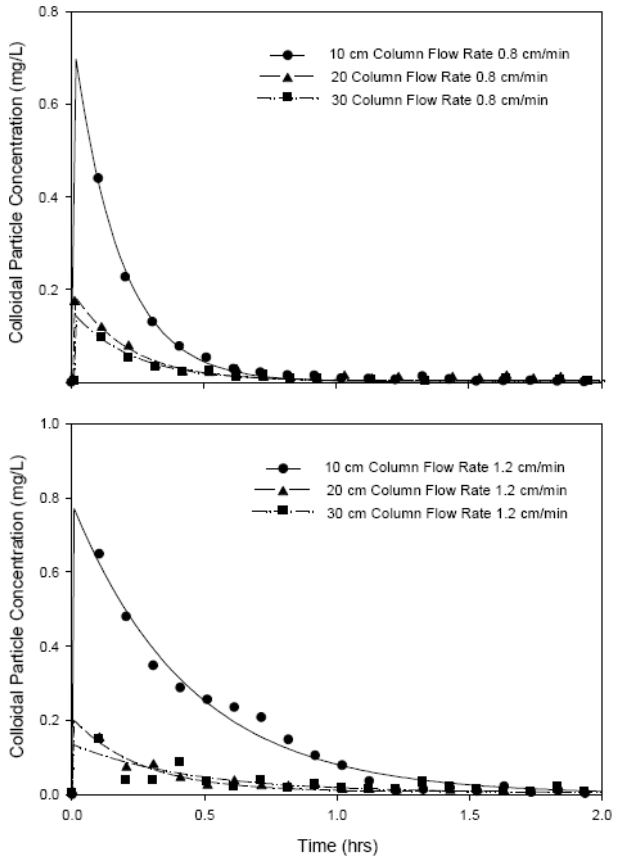

Fig 3. Colloidal Particle Release and Breakthrough Curves.

In this research, colloidal particle release and mobilization curves were simulated against **Eqs (5)** and **(6)** using Hydrus-1D with variable colloidal particle release rate coefficient and deposition rate coefficient for each sensor section. Hydrus-1D is an implicit, finite-difference scheme, which optimizes colloidal particle release rate coefficient and deposition rate coefficient by minimizing the sum of squared differences between observed and fitted data using the nonlinear least-squares method (Toride *et al.*, 1995). The simulation process was based on the assumption that colloidal particle release and deposition occurred simultaneously and kinetically with colloidal particle release rate coefficient and deposition rate coefficient being constant within the section of the sensor. Consequently, colloidal particle release rate coefficient and deposition rate coefficient varied for each 10-cm of the column depth.

Along the length of the columns, released colloidal particles were subject to subsequent retention during transport. More colloidal particles were released at the top of the columns as compared with that of the bottom as demonstrated by greater colloidal particle release rate coefficients (**Fig. 4**). At the same time, less colloidal particles were retained at the top of the columns as compared with that of the bottom as demonstrated by smaller deposition rate coefficients (**Fig. 5**). Above observations directly resulted from the fact that the top section of the columns had greater water saturation than the bottom section of the columns. Owing to the overall greater water contents, the shorter-length columns had more colloidal particles released than the long-length columns. In addition, released colloidal particles suffered less retention in the shorter-length columns. Consequently, the shorter-length columns manifested higher peak concentrations (**Fig. 3**). By integrating the colloidal particle release and mobilization curves, the accumulative amount of colloidal particles released for each column was calculated. Accordingly, the accumulative amount of colloidal particles released decreased with the increase of the column length.

Colloidal particle deposition was controlled by the air-water interface. From the top to the bottom of the columns, effective saturation decreased. Accordingly, along the depth of the sediment columns, the air-water interface increased owing to the decrease of water content. Colloidal particles thus suffered greater deposition.

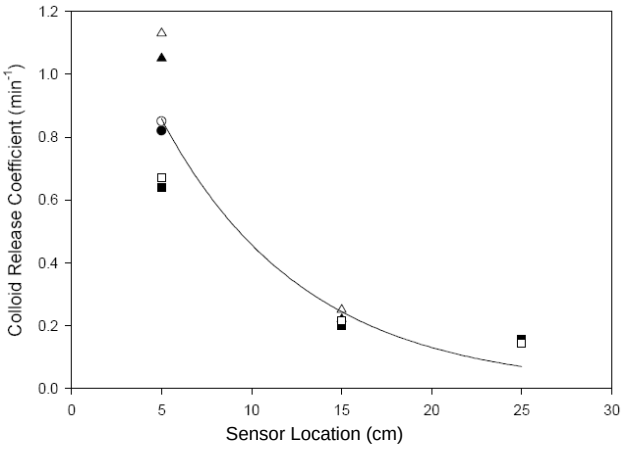

Fig 4. Colloid Release Rate Coefficient as a Function of Column Length.

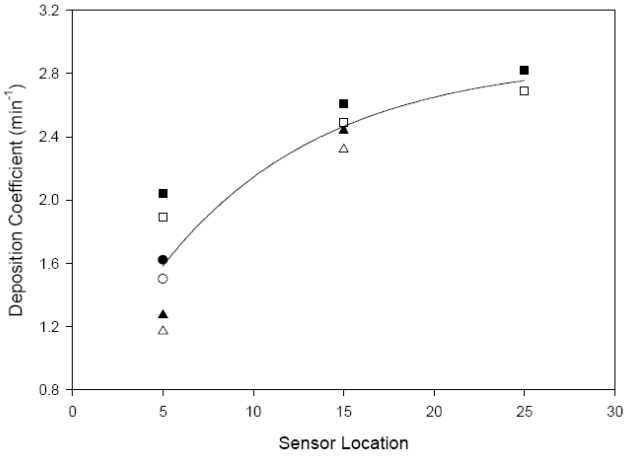

Fig 5. Colloid Deposition Rate Coefficient as a Function of Column Length.

The deposition of the colloidal particles manifested an exponential increase with the decrease of system water saturation for the range of our experiments. The air-water interface, which plays a key role in controlling colloidal particle retention under water unsaturated conditions, can be estimated from the pore size radii using **Eq. (7)** (Cary, 1994):

$$S_0 = \frac{\rho_0 g}{\alpha\gamma}\int_{\theta}^{\theta_0}[(\frac{\theta}{\theta_0})^{\frac{n}{1-n}} - 1]^{\frac{1}{n}}\,d\theta \qquad (7)$$

where S_0 is the air-water interfacial area (cm^2/cm^3), ρ is the water density (kg/m^3), g is the gravitational constant (9.8 m/s^2), γ is the water surface tension (72.69 mJ/m^2 at 20°C), and θ_0 is the porous medium's volume fraction of pore space or porosity of the column. The variables α and n are defined previously.

In this research, all the column experiments were conducted at water saturation ranging from 0.4 to 0.8, within which the air-water interfacial area displayed a linear relationship with water saturation. The increase of colloidal particle deposition with decreasing water saturation should show the same trend as with that of increasing air-water interfacial area. To reflect increased colloidal particle retention with decreasing water saturation, colloidal particle deposition rate coefficients were plotted against the air-water interface (**Fig. 6**). The linear relationship indicated that the increased colloidal particle retention was attributed to the increased air-water interface. Colloidal particle release was also found to be a function of effective water saturation. With the increase of water saturation, colloidal particle release increased exponentially (**Fig. 7**).

Under water unsaturated conditions, the capillary force, F_{cap}, is the dominating force exerted on colloidal particles and can be calculated following **Eq. (8)**:

$$F_{cap} = \pi R\gamma[2\sin\phi\sin(\varphi+\phi) + \cos\varphi(1+\cos\phi)^2 - \sin\phi] \qquad (8)$$

where ϕ is the filling angle (degree) between the center of the colloidal particle (assuming spherical shape) and the water-colloidal particle contact line, φ is the water contact angle (degree). In addition to the capillary force, colloidal particles also experienced electrostatic, Lifshitz-van der Waals, and Lewis acid-base interactions with the sediments and the air-water interface. Since colloidal particles, sediments and the air-water interface were all negatively charged, electrostatic interactions between colloidal particles and the sediments and between colloidal particles and the air-water interface were repulsive (Graciaa *et al.*, 1995). The repulsive electrostatic interactions operated in the range of several tens of nanometers. At the equilibrium distance where colloidal particles contacted the sediment surface, electrostatic interactions could be ignored owing to superimposition of the double layers, and Lifshitz-van der Waals and Lewis acid-base interactions overshadowed the electrostatic interactions.

The capillary force was one order of magnitude greater than Lewis acid-base interactions, two orders of magnitude greater than Lifshitz-van der Waals interactions, and four orders of magnitude greater than electrostatic interactions when evaluated at the equilibrium distance. Thus, capillary force controlled colloidal particle release in unsaturated systems. With the increase of water saturation, capillary force decreased owing to the increase of the filling angle. Colloidal particle release rate coefficient increased with the decrease of capillary force (**Fig. 8**).

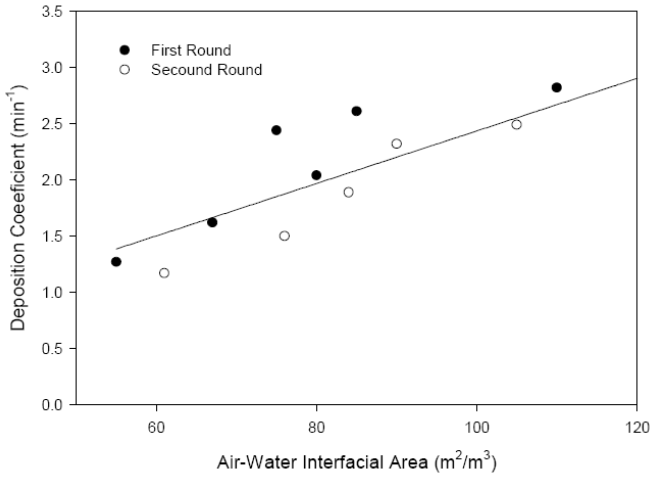

Fig 6. Colloid Release Rate Coefficient as a Function of Air-Water Interfacial Area

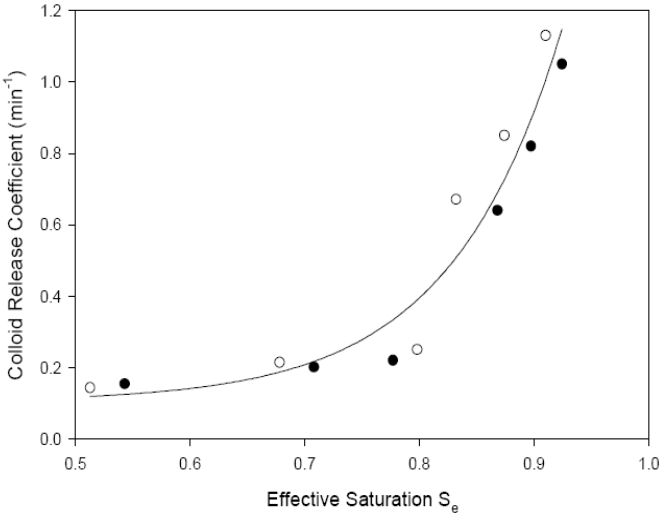

Fig 7. Colloid Particle Release Rate Coefficient as a Function of Water Saturation

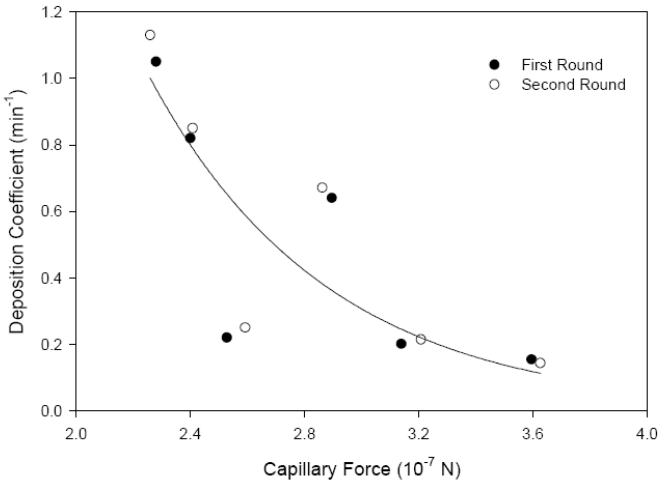

Fig 8. Colloidal Particle Release Rate Coefficient as a Function of Capillary Force

CONCLUSIONS

In this research, intact sediment column experiments were conducted to examine colloid release from different soil depth. It was found that more colloidal particles were found to be released at the top of the columns as compared with that of the bottom, which was closely linked to water saturation. Owing to the overall greater water contents, the shorter-length columns had more colloidal particles released than the long-length columns. It was concluded in this research that release of in situ colloidal particles from sediments was a function of sediment depth, resulted from water saturation variation along the length of the sediments. In addition, the capillary force was discovered to play an important role in controlling colloid release. With the increase of water saturation, capillary force decreased owing to the increase of the filling angle, colloidal particle release rate coefficient increased accordingly.

Acknowledgment The work was supported by the National Research Initiative of the USDA Cooperative State Research, Education and Extension Service, Grant No. 2007-35102-18111 to Florida A&M University.

REFERENCES

Bergendahl J., Grasso D. (2000): Prediction of colloid detachment in a model porous media: Hydrodynamics. Chemical Engineering Science, 55: 1523–1532.

Bin G., Cao X.D., Dong Y., Luo Y.M., Ma L.Q. (2011): Colloid deposition and release in soils and their association with heavy metals. Critical Reviews in Environmental Science and Technology, 41: 336–372.

Bolshov L.A., Kondratenko P.S., Matveev L.V. (2011): Colloid-facilitated contaminant transport in fractal media. Physical Review E, 84: DOI:10.1103/PhysRevE.84.041140.

Bradford S.A., Simunek J., Bettahar M., van Genuchten M.T., Yates S.R. (2003): Modeling colloid attachment, straining, and exclusion in saturated porous media. Environmental Science & Technology, 37: 2242–2250.

Bradford S.A., Toride N. (2007): A stochastic model for colloid transport and deposition. Journal of Environmental Quality, 36: 1346–1356.

Bradford S.A., Yates S.R., Bettahar M., Simunek J. (2002): Physical factors affecting the transport and fate of colloids in saturated porous media. Water Resources Research, 38: 1327 –1338.

Cary J.W. (1994): Estimating the surface area of fluid phase interfaces in porous media. Journal of Contaminant Hydrology, 15: 243–248.

Chen G., Flury M., Harsh J.B., Lichtner P.C. (2005): Colloid-facilitated transport of cesium in variably saturated Hanford sediments. Environmental Science & Technology, 39: 3435 – 3442.

Graciaa A., Morel G., Saulner P., Lachaise J., Schechter R.S. (1995): The potential of gas-bubbles. Journal of Colloid and Interface Science, 172: 131–136.

Gravelle A., Peysson Y., Tabary R., Egermann P. (2011): Experimental investigation and modelling of colloidal release in porous media. Transport in Porous Media, 88: 441–459.

Lenhart J.J., Saiers J.E. (2002): Transport of silica colloids through unsaturated porous media: Experimental results and model comparisons. Environmental Science & Technology, 36: 769–777.

Lenhart J.J., Saiers J.E. (2003): Colloid mobilization in water-saturated porous media under transient chemical conditions. Environmental Science & Technology, 37: 2780–2787.

Li, X.Q. Scheibe T.D., Johnson W.P. (2004): Apparent decreases in colloid deposition rate coefficients with distance of transport under unfavorable deposition conditions: A general phenomenon. Environmental Science & Technology, 38: 5616–5625.

McCarthy J.F., Shevenell L. (1998): Processes controlling colloid composition in a fractured and karstic aquifer in eastern Tennessee, USA. Journal of Hydrology, 206: 191–218.

Molin S., Cvetkovic V. (2010): Microbial risk assessment in heterogeneous aquifers: 1. Pathogen transport. Water Resources Research, 46: W05518.

Molin, S. Cvetkovic V., Stenstrom T.A. (2010): Microbial risk assessment in heterogeneous aquifers: 2. Infection risk sensitivity. Water Resources Research, 46: W05519.

Roy S.B., Dzombak D.A. (1996): Colloid release and transport processes in natural and model porous media. Colloids and Surfaces A: Physicochemical and Engineering Aspects, 107: 245–262.

Ryan J., Gschwend P.M. (1994): Effect of ionic strength and flow rate on colloid release: Relating kinetics to inter-surface potential energy. Journal of Colloid and Interface Science, 164: 21–34.

Sen T.K. (2011): Processes in pathogenic biocolloidal contaminants transport in saturated and unsaturated porous media: A review. Water, Air, & Soil Pollution, 216: 239–256.

Shang J.Y., Flury M., Chen G., Zhuang J. (2008): Impact of flow rate, water content, and capillary forces on in situ colloid mobilization during infiltration in unsaturated sediments. Water Resources Research, 44: W06411.

Sharma M.M., Chamoun H., Sarma D.S.H.S.R., Schechter R.S. (1992): Factors controlling the hydrodynamic detachment of particles from surfaces. Journal of Colloid and Interface Science, 149: 121–134.

Sharma P., Flury M., Mattson E.D. (2008): Studying colloid transport in porous media using a geocentrifuge. Water Resources Research, 44: W07407.

Shen C.Y., Li B.G., Huang Y.F., Jin Y. (2007): Kinetics of coupled primary- and secondary-minimum deposition of colloids under unfavorable chemical conditions. Environmental Science & Technology, 41: 6976–6982.

Thomas J.M., Chrysikopoulos C.V. (2010): A new method for in situ concentration measurements in packed-column transport experiments. Chemical Engineering Science, 65: 4285–4292.

Thompson M.L., Scharf R.L. (1994): An improved zero-tension lysimeter to monitor colloid transport in soils. Journal of Environmental Quality, 23: 378–383.

Toride N., Leij F.J., van Genuchten M.T. (1995): The CXTFIT code for estimating transport parameters from laboratory or field experiments, Version 2.1, U.S. Salinity Laboratory: Riverside, CA.

Tufenkji N., Redman J.A., Elimelech M. (2003): Interpreting deposition patterns of microbial particles in laboratory-scale column experiments. Environmental Science & Technology, 37: 616–623.

Vendelboe A.L., Moldrup P., Heckrath G., Jin Y., de Jonge L.W. (2011): Colloid and phosphorus leaching from undisturbed soil cores sampled along a natural clay gradient. Soil Science, 176: 399–406.